AIP Advances

Effect of layer thickness on device response of silicon heavily supersaturated with sulfur

David Hutchinson, Jay Mathews, Joseph T. Sullivan, Austin Akey, Michael J. Aziz, Tonio Buonassisi, Peter Persans, and Jeffrey M. Warrender

Citation: AIP Advances **6**, 055307 (2016); doi: 10.1063/1.4948986
View online: http://dx.doi.org/10.1063/1.4948986
View Table of Contents: http://scitation.aip.org/content/aip/journal/adva/6/5?ver=pdfcov
Published by the AIP Publishing

Effect of layer thickness on device response of silicon heavily supersaturated with sulfur

David Hutchinson,[1,2] Jay Mathews,[3,4] Joseph T. Sullivan,[5] Austin Akey,[5,6] Michael J. Aziz,[6] Tonio Buonassisi,[5] Peter Persans,[1] and Jeffrey M. Warrender[3,a]

[1]*Department of Physics, Applied Physics, and Astronomy, Rensselaer Polytechnic Institute, Troy NY 12180, USA*
[2]*Department of Physics and Nuclear Engineering, United States Military Academy, West Point NY 10996, USA*
[3]*US Army ARDEC – Benét Laboratories, Watervliet NY 12189, USA*
[4]*Department of Physics, University of Dayton, Dayton, OH 45469, USA*
[5]*School of Engineering, Massachusetts Institute of Technology, Cambridge MA 02139, USA*
[6]*Harvard John A. Paulson School of Engineering and Applied Sciences, Cambridge MA 02138, USA*

(Received 22 February 2016; accepted 28 April 2016; published online 5 May 2016)

We report on a simple experiment in which the thickness of a hyperdoped silicon layer, supersaturated with sulfur by ion implantation followed by pulsed laser melting and rapid solidification, is systematically varied at constant average sulfur concentration, by varying the implantation energy, dose, and laser fluence. Contacts are deposited and the external quantum efficiency (EQE) is measured for visible wavelengths. We posit that the sulfur layer primarily absorbs light but contributes negligible photocurrent, and we seek to support this by analyzing the EQE data for the different layer thicknesses in two interlocking ways. In the first, we use the measured concentration depth profiles to obtain the approximate layer thicknesses, and, for each wavelength, fit the EQE *vs.* layer thickness curve to obtain the absorption coefficient of hyperdoped silicon for that wavelength. Comparison to literature values for the hyperdoped silicon absorption coefficients [S.H. Pan *et al*. Applied Physics Letters **98**, 121913 (2011)] shows good agreement. Next, we essentially run this process in reverse; we fit with Beer's law the curves of EQE *vs.* hyperdoped silicon absorption coefficient for those wavelengths that are primarily absorbed in the hyperdoped silicon layer, and find that the layer thicknesses obtained from the fit are in good agreement with the original values obtained from the depth profiles. We conclude that the data support our interpretation of the hyperdoped silicon layer as providing negligible photocurrent at high S concentrations. This work validates the absorption data of Pan *et al*. [Applied Physics Letters **98**, 121913 (2011)], and is consistent with reports of short mobility-lifetime products in hyperdoped layers. It suggests that for optoelectronic devices containing hyperdoped layers, the most important contribution to the above band gap photoresponse may be due to photons absorbed below the hyperdoped layer. [http://dx.doi.org/10.1063/1.4948986]

INTRODUCTION

The incorporation of greater-than-equilibrium concentrations of sulfur into silicon *via* laser surface structuring[2] and ion implantation and pulsed laser melting (II-PLM)[3] has attracted interest over the last several years due to the observation of sub gap optical absorption[4–6] and device

[a]Corresponding author. Electronic mail jwarrend@post.harvard.edu

response.[7] The optoelectronic properties of the II-PLM material have been studied as well.[8,9] Relatively less work has been done on the above-band gap optoelectronic properties of this material, in part because the strong contribution to the absorption made by the substrate makes isolation of the II-PLM layer challenging. Recently, a careful experimental investigation used the II-PLM method to incorporate S into the device layer of a silicon-on-insulator (SOI) wafer, and then chemically etched a "window" in the handle wafer to permit measurement of the S-doped layer without the substrate. This enabled measurement of the above-gap absorption of the S-doped layer.[1] The results showed that the absorption coefficient of the S-doped layer exceeds that of a standard Si wafer. Subsequent work used these absorption coefficients to analyze coplanar measurements on II-PLM SOI layers.[10,11]

Hyperdoped silicon layers fabricated by the method described in Ref. 4 are on the order of a few hundred nanometers thick. If we invert the wavelength-dependent absorption coefficients from Ref. 1 to obtain absorption lengths, we find that the numbers so obtained are comparable to the layer thickness. Thus, much of the visible light incident on the sample, particularly in the blue and green regions of the spectrum, is absorbed in the S-rich layer. In this paper, we report on an experimental investigation into a set of devices made using the II-PLM method, in which the S concentration is kept approximately constant and the S layer thickness is changed.

First, we assume (based on secondary ion mass spectrometry data) that we know the approximate thickness of these layers, and show how the measured external quantum efficiencies for photons that are absorbed below the S layer are internally consistent with the absorption data of Ref. 1. Next, we show how the measured external quantum efficiencies for photons that are absorbed within the S layer are also consistent with this picture, and are internally consistent with the assumed layer thicknesses. These observations suggest that, for above-band gap photons, the optoelectronically relevant absorption occurs below the junction in the Si sublayer. Therefore, the most important function of the sulfur layer at these high concentrations, with respect to device performance, is primarily electronic rather than optical in nature.

EXPERIMENTAL

p-type silicon (100) wafers, resistivity 1-10 Ω-cm, were ion-implanted with ^{32}S (Cutting Edge Ions) at three different energies and implantation doses as shown in Table I, so as to give three different peak ion ranges but approximately equal average S concentration after subsequent laser processing. Pieces of these wafers were then pulsed laser melted with a spatially-homogenized XeCl excimer laser (Questek), with concurrent time resolved reflectivity using an argon ion laser to monitor melt duration. The laser spot was approximately 3×3 mm^2, and each area of the sample received one (1) laser shot. The laser fluence was varied with the implantation conditions, with higher fluence supplied to the sample that received the higher implantation energy (deeper implant). The desired fluence for each sample was chosen from the results of one-dimensional heat flow and impurity diffusion calculations, described elsewhere.[4,15,16] Several areas were irradiated on each sample at varying fluence, and the samples chosen for subsequent analysis were those that collectively exhibited the most similar S concentrations in secondary ion mass spectrometry (SIMS) profiles, although the range of variation over the samples was small. The fluences used to fabricate the samples discussed in this work are given in Table I.

TABLE I. Parameters used in fabrication of the samples, and measured/calculated for those samples.

Implant energy (keV)	^{32}S dose (at./cm^2)	Laser fluence (J/cm^2)	Average S concentration (at./cm^3)	Layer thickness (nm) (S content $>10^{19}$ at./cm^3)	Threshold wavelength (nm)
40	7.5×10^{15}	1.7	2.9×10^{20}	235	445
95	1×10^{16}	1.7	1.7×10^{20}	410	480
140	1.5×10^{16}	2.0	2.2×10^{20}	525	515

Metal contacts were evaporated on front and back surfaces using an electron-beam evaporator. Front contacts were a stack of Ti/Ni/Ag and formed an interdigitated pattern. The rear contacts were square aluminum pads. More details are described in previous literature.[7]

Three contacted devices were prepared for each fluence, and these were each measured in a spectral responsivity measurement setup, described elsewhere.[10] Briefly, mechanically chopped light from a tungsten filament lamp is directed through a grating monochromator, with a spectral width of about 5nm, onto the sample. The sample contacts are connected to a lock-in amplifier in series with a 1 kΩ resistor, with a voltage applied across the circuit such that the sample, which acts as a photodiode, is in reverse bias. A computer program reads out and stores the signal from the lock-in as the wavelength is swept from 400 to 700 nm. The dark signal is measured and subtracted uniformly from the measured spectrum for each sample. The lamp spectrum is separately measured using a calibrated silicon photodiode (ThorLabs), and the measured spectrum for each sample is divided by the result. External quantum efficiency as a function of wavelength λ was calculated according to the well-known relationship, $\mathrm{EQE}(\lambda) = R(\lambda)\, h\, c/(\lambda\, e)$, where R is the measured spectral responsivity at that wavelength, h is Planck's constant, c the speed of light, and e the electron charge.

Some of the contacted devices exhibited anomalously high external quantum efficiency, which is attributed to a phenomenon described elsewhere.[12] One indicative feature is the highly localized nature of this anomalously high EQE when the sample is placed into an EQE mapping setup.[12] None of the samples used in this paper showed this high EQE in mapping measurements.

RESULTS AND DISCUSSION

In Fig. 1, we present the SIMS depth profiles for the post-laser melted layers. We identify the depth at which each sample crosses a sulfur concentration of 10^{19} at/cm^3 as defining the thickness of

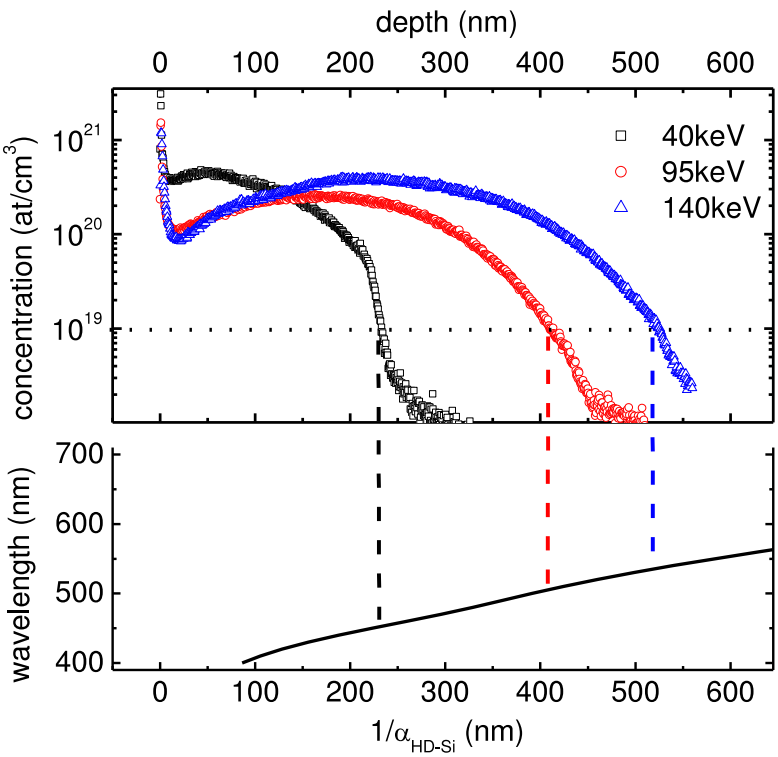

FIG. 1. (top) SIMS concentration depth profiles after laser melting. The horizontal line indicates a concentration of 10^{19} at./cm^3 (bottom) Wavelength *vs*. "Penetration depth" ($1/\alpha_{\mathrm{HD-Si}}$) using measured values for $\alpha_{\mathrm{HD-Si}}$ from Ref. 1. Vertical lines from the top panel intersect the curve of the bottom panel, giving rise to the "critical wavelength" for each sample.

the S-rich layer. Although there is S deeper than this in the Si, we note that greater than 99.5% of the S is contained in the layer above this depth. According to Fig. 6 of Ref. 4, the absorption coefficient at this concentration is about 10% of the peak absorption for wavelengths between 1130-2070nm. According to Fig. 3 in Ref. 1, a sample with average S concentration of 1.5×10^{20} at/cm^2 absorbs approximately 3-4 times more in the visible than a sample having average S concentration of 2×10^{19} at/cm^2. The results that will be presented will further validate this choice for the layer thickness.

Using the absorption data from Fig. 3 of Ref. 1, we can calculate the $1/\alpha$ "absorption length" of a S-rich layer comparable to the one that Pan *et al.* studied, i.e., a layer having an average S concentration of about 1.5×10^{20} at/cm^3.[13] This is plotted in the bottom panel of Fig. 1 with the ordinate as the wavelength, and the abscissa aligned with the depth axis of the upper panel. Thus, extending lines down from the 10^{19} at./cm^3 depth for each of the three samples, we can use the bottom panel to obtain a "threshold wavelength". For shorter wavelengths, most of the incident light would be expected to be absorbed in the S-rich layer, and for longer wavelengths, a significant fraction of the light would be expected to penetrate through to the substrate.

This figure reveals that, for above-band gap measurements in Si:S devices, much of the relevant absorption happens in the underlying Si substrate, and not in the Si:S layer, for all but the shortest visible wavelengths.

Next, we examined the EQE as a function of penetration depth into the silicon sublayer, using published data for the silicon absorption coefficient[14] to obtain the penetration depth. In Fig. 2 we show the measured EQE for the three samples as a function of penetration depth into the silicon; the corresponding wavelengths are shown on the top axis.

We now impose an interpretive framework in which we assume that the S-rich layer contributes no meaningful photoresponse for illumination in the range between 400-700nm. In this framework, the only significant difference between the layers comes from their increasing thickness, with the thicker layers providing correspondingly more attenuation of the incident light. This framework is motivated by observations of low mobility-lifetime ($\mu\tau$) product in Si:S layers.[9,10] We assume, following Pan *et al.*, that the S concentration can be treated as approximately uniform, and that the layer thicknesses are as shown in Table I. With these assumptions, we can, at each penetration depth (i.e., each incident wavelength), draw a line plotting the natural logarithm of the EQE for the three

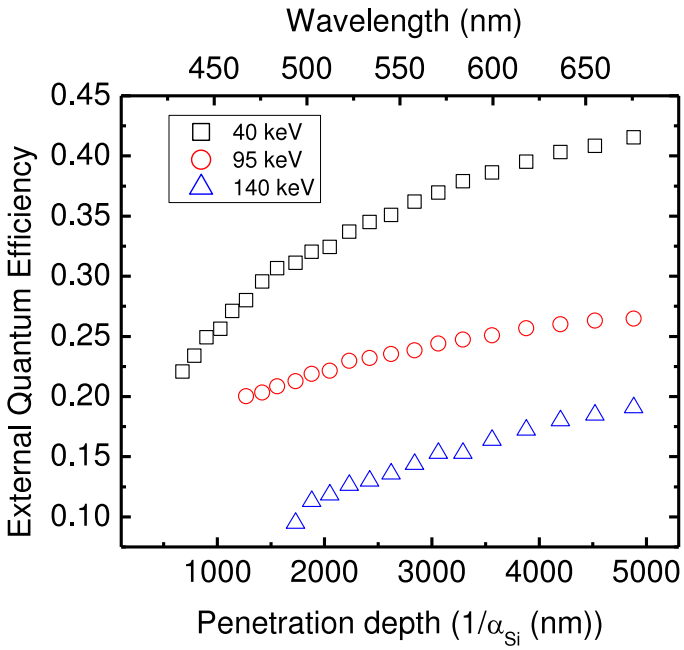

FIG. 2. Measured external quantum efficiency (EQE) *vs.* $1/\alpha_{Si}$, penetration length into the sublayer silicon.

samples against their layer thicknesses. If our interpretive framework is correct, the slope of that line should be the absorption coefficient of hyperdoped silicon. Even though we are evaluating light that has passed through the hyperdoped silicon layer, it is the hyperdoped silicon layer that is doing the attenuating. For a photon that reaches the sublayer, there should be no further differences between the samples in the subsequent propagation and absorption of that wavelength. To test whether this is indeed the case, we plot the experimental values of α we obtained for each wavelength *vs.* α_{HD-Si} (the absorption coefficient for hyperdoped Si from Ref. 1 for that same wavelength), and fit a line to this. We show the result in Fig. 3. The slope of the line fit is close to -1, with an R^2 (goodness of fit) value of 0.987; thus, this fit is consistent with our interpretive framework.

As a further demonstration of the consistency of our interpretive framework with the measured quantum efficiencies, we start with the assumption that the hyperdoped silicon absorption coefficients of Ref. 1 are correct, and see whether we can obtain layer thicknesses comparable to the values from Fig. 1 when we consider the wavelengths for which absorption occurs primarily within the Si:S layer. As Fig. 4 shows, we can plot the EQE as a function of hyperdoped silicon absorption coefficient α_{HD-Si} and fit to a simple exponential, $y = y_0 + A\exp[-\alpha_{HD-Si}\, d]$, where y_0, A, and d are the fit parameters. Here, we are fitting the curve for each sample individually, and we expect that, if our interpretive framework holds, the signal should simply decrease with wavelength according to Beer's law. For each fit, we extend the range of the fit (indicated by vertical bars) to 40nm past the cutoff wavelength both to allow for better statistics and to prevent our selection of the cutoff wavelength (a consequence of our selection of the threshold concentration) from influencing the fit too heavily. As a comparison, for 40keV, when we change the upper limit of the fit from 485nm to 445nm, the resulting thickness changes by only about 5%, but the overall quality of the fit is slightly worse, with the R^2 value of the fit decreasing from 0.99 to 0.96. Also, for the 140keV sample, we excluded EQE data below 465nm (α_{HD-Si} = 0.00371 nm^{-1}), as these go below zero and are thus considered to be within the measurement noise. (The noise in the blue portion of the spectrum, observed in all measurements, is partially attributable to the decrease of the W lamp source intensity in that wavelength range. A brighter source in the blue could provide better data). The parameters for all fits are presented in Table II. The best-fit thicknesses are 277, 395, and 740nm for the 40, 95, and 140keV samples, respectively.

It should be noted that this fit contains two free parameters, y_0 and A, which are reasonably comparable for all three samples; for example, if we alter the value of A for the 95keV sample by forcing it to the value of the 40keV sample, the calculated thickness becomes 467nm instead of 395nm. So, this suggests an error in the fit thicknesses of about 20%.

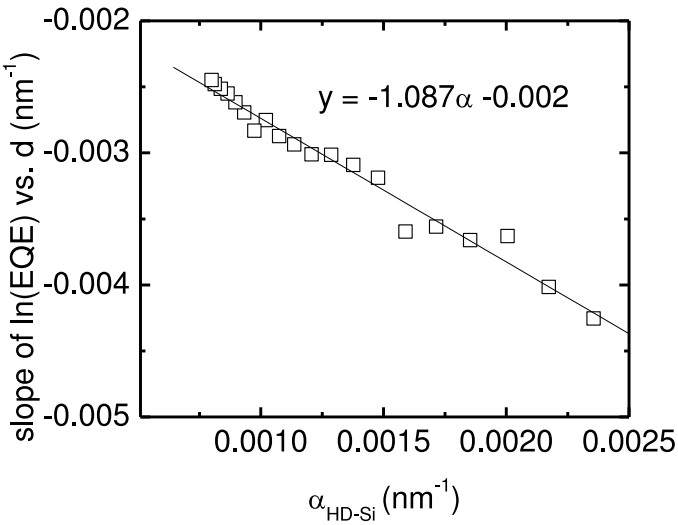

FIG. 3. α_{HD-Si} obtained from fits of ln(EQE) *vs.* layer thickness as a function of wavelength, *vs.* α_{HD-Si} from Ref. 1. A linear fit shows a slope that is close to -1, indicating good agreement between the absorption coefficients obtained in this work and the literature values.

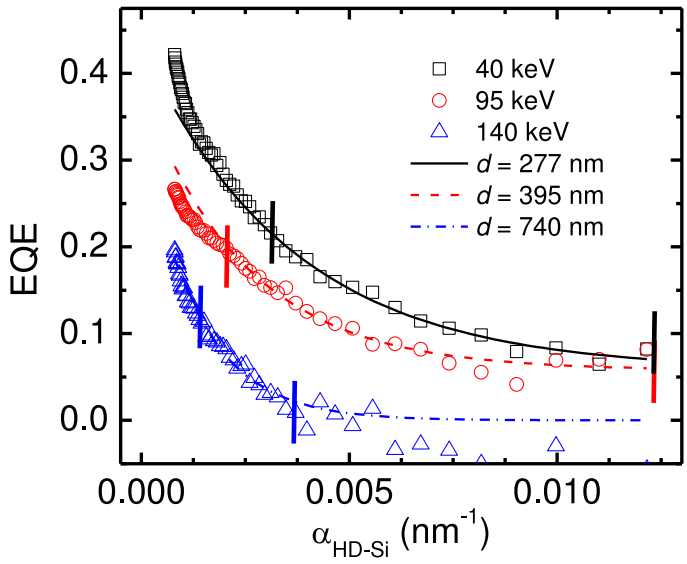

FIG. 4. EQE *vs.* α_{HD-Si} values from Ref. 1. Fits of $y = y_0 + A \exp[-\alpha_{HD-Si} d]$ are shown as lines; the legend shows the best-fit values of d obtained from the fits. The vertical bars bound the range of α_{HD-Si} over which the fits were performed.

A more rigorous, two-parameter, fit can be obtained by fitting the natural logarithm of the EQE *vs.* α_{HD-Si}; in this case, the resulting thicknesses are 198, 234, and 734nm for 40, 95, and 140 keV, respectively.[17] Both of these fitting schemes show a slightly greater thickness for the 140 keV layer than the initial estimate from Fig. 1 would have suggested, and well beyond the depth at which non-negligible levels of S can be detected. This suggests that, according to the EQE measurement, there may be more absorption than we would expect from the thicker layer. One possible explanation may be that damage to the surface associated with the higher fluence has occurred, although we did not specifically observe this upon visual inspection. It is also possible that the lower signal relative to the noise floor for this sample has introduced error in the measurement at these shorter wavelengths.

The functional form used in these fits reflects the underlying interpretive framework we have imposed all along, in which the S-rich layer acts primarily as an absorbing layer. If instead the S layer was contributing appreciably to the photoresponse, we would expect a flat spectral profile. Although surface recombination may account for some signal decay at short wavelengths, we would have expected a similar signal magnitude and decay for all three layers in this spectral region if significant photocurrent was generated in the S layer. The diminished signal at increasing S layer thickness indicates that what photoresponse does occur at these wavelengths is due to the light that penetrates to the substrate. As the S layer thickness increases, so little short-wavelength light gets through that there is essentially no photoresponse, and the measured quantum efficiency is in the noise floor of the measurement.

In conclusion, we see, especially for the 40keV and 95keV samples, good agreement between the thickness values obtained from Beer's law fits of the EQE *vs.* α_{HD-Si} spectra of the S-rich layer (using Pan's α_{HD-Si} values) and those thicknesses that we posited from the beginning based on

TABLE II. Fit parameters for exponential fits to EQE *vs.* α_{HD-Si} for absorption in the S-rich layer.

Sample	y_0	A	d (nm)	R^2
40 keV	0.058	0.38	277	0.99
95 keV	0.058	0.32	395	0.96
140 keV	0[a]	0.34	740	0.98

[a]y_0 was forced to 0 for the 140 keV sample.

the SIMS data. Separately, we found that using Beer's law fits to calculate the α_{HD-Si} from EQE measurements in the Si sublayer, given thickness values obtained from SIMS, produced values of α_{HD-Si} that were in excellent agreement with Pan's values. We have therefore shown that the data are consistent with the interpretive framework we posited, in which the primary role of the S layer, optically speaking, is to merely attenuate the incident light for above-band gap photons without contributing any photo-generated carriers. This is likely attributable to the low $\mu\tau$ product characteristic of these layers.[10] For sub band gap photons, the behavior may not be very different, as the $\mu\tau$ is equally low.[18] However, for different impurities or different S concentrations, these same observations may not hold. Additionally, alternative strategies such as co-doping with a compensating impurity[19] may yield different responsivity behavior.

The framework established in this paper may prove useful in evaluating the relative unimportance of the impurity-rich layer compared to that of the sublayer in determining the photoresponse of the device. And in any case, given absorption coefficients in the range of those reported by Pan *et al*., it must be considered that the majority of visible and near-infrared light absorbed by the sample is absorbed below the impurity-rich layer. Thus, analysis of the electronic function of the impurity-rich layer, as the layer on the opposite side of the *p-n* junction from where the photocarriers are generated, will be important in understanding the photoresponse spectra for above-band gap photons incident on laser-doped silicon. Additionally, studies seeking to quantify the transport properties of hyperdoped layers can take advantage of this effect by selecting optical probe wavelengths that maximize absorption in the layer in which one wishes to generate photocarriers.

ACKNOWLEDGEMENTS

We gratefully acknowledge Michael Magaletta for data collection, Daniel Recht for technical assistance, and Harry Efstathiadis and Girish Malladi of SUNY Polytechnic Institute(NY) for Rutherford backscattering spectrometry data. This work was partially supported by funding through the Army Research Laboratory's Institute for Soldier Nanotechnology.

[1] S.H. Pan, D. Recht, S. Charnvanichborikarn, J.S. Williams, and M.J. Aziz, Applied Physics Letters **98**, 121913 (2011).
[2] C.H. Crouch, J.E. Carey, J.M. Warrender, M.J. Aziz, E. Mazur, and F.Y. Génin, Applied Physics Letters **84**, 1850 (2004).
[3] T.G. Kim, J.M. Warrender, and M.J. Aziz, Applied Physics Letters **88**, 241902 (2006).
[4] B.P. Bob, A. Kohno, S. Charnvanichborikarn, J.M. Warrender, I. Umezu, M. Tabbal, J.S. Williams, and M.J. Aziz, Journal of Applied Physics **107**, 123506 (2010).
[5] I. Umezu, J.M. Warrender, S. Charnvanichborikarn, A. Kohno, J.S. Williams, M. Tabbal, D.G. Papazoglou, X.-C. Zhang, and M.J. Aziz, Journal of Applied Physics **113**, 213501 (2013).
[6] I. Umezu, A. Kohno, J.M. Warrender, Y. Takatori, Y. Hirao, S. Nakagawa, A. Sugimura, S. Charnvanichborikarn, J.S. Williams, and M.J. Aziz, American Institute of Physics Conference Proceedings **1399**, 51 (2011).
[7] A.J. Said, D. Recht, J.T. Sullivan, J.M. Warrender, T. Buonassisi, P.D. Persans, and M.J. Aziz, Applied Physics Letters **99**, 073503 (2011).
[8] M. Tabbal, T.G. Kim, J.M. Warrender, M.J. Aziz, B.L. Cardozo, and R.S. Goldman, Journal of Vacuum Science and Technology B **25**, 1947 (2007).
[9] D. Recht, D. Hutchinson, T. Cruson, A. DiFranzo, A. McAllister, A.J. Said, J.M. Warrender, P.D. Persans, and M.J. Aziz, Applied Physics Express **5**, 041301 (2012).
[10] P.D. Persans, N.E. Berry, D. Recht, D. Hutchinson, H. Peterson, J. Clark, S. Charnvanichborikarn, J.S. Williams, A. DiFranzo, M.J. Aziz, and J.M. Warrender, Applied Physics Letters **101**, 111105 (2012).
[11] P.D. Persans, N.E. Berry, D. Recht, D. Hutchinson, A.J. Said, J.M. Warrender, H. Peterson, A. DiFranzo, C. McGahan, J. Clark, W. Cunningham, and M.J. Aziz, Materials Research Society Symposium Proceedings **1321** (2011).
[12] Persans *et al.*, manuscript preparation in progress.
[13] The comparison plot shown in Fig.3 of Ref. 1 shows that, in the wavelength range from 400-700nm, the data taken by Pan *et al*. for an average concentration of 1.5×10^{20} at/cm^2 is indistinguishable from the data in Ref. 4, which was emulated in this study. The samples in the former were fabricated on silicon-on-insulator substrates and in latter, on bulk silicon.
[14] M.A. Green and M.J. Keevers, Progress in Photovoltaics **3**, 189 (1995).
[15] D.E. Hoglund, M.O. Thompson, and M.J. Aziz, Physical Review B **58**, 189 (1998).
[16] R. Reitano, P.M. Smith, and M.J. Aziz, Journal of Applied Physics **76**, 1518 (1994).
[17] D. Hutchinson, Ph.D. thesis, Rensselaer Polytechnic Institute, Troy, NY (2014).
[18] J.T. Sullivan, C.B. Simmons, J.J. Krich, A.J. Akey, D. Recht, M.J. Aziz, and T. Buonassisi, Journal of Applied Physics **114**, 103701 (2013).
[19] C.B. Simmons, A.J. Akey, J.P. Mailoa, D. Recht, M.J. Aziz, and T. Buonassisi, Advanced Functional Materials **24**, 2852 (2014).